INFN/AE–97/05
24 Gennaio 1997

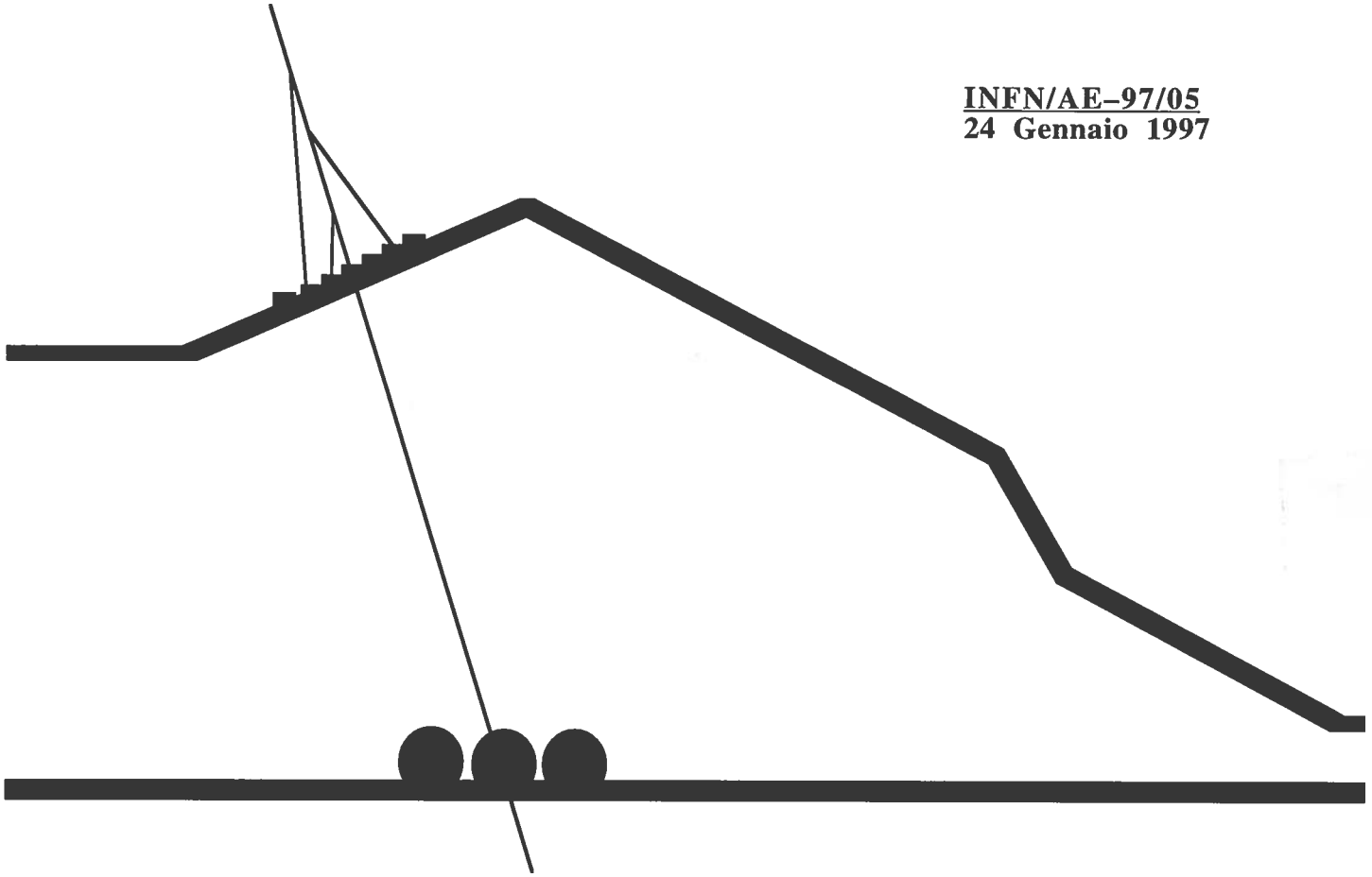

Seasonal Variations in the Underground Muon Intensity as Seen by MACRO

The MACRO Collaboration

INFN - Laboratori Nazionali del Gran Sasso

Published by ***SIS–Pubblicazioni***
dei Laboratori Nazionali di Frascati

INFN – Istituto Nazionale di Fisica Nucelare
Laboratori Nazionali del Gran Sasso

INFN/AE–97/05
24 Gennaio 1997

Seasonal Variations in the Underground Muon Intensity as Seen by MACRO

the MACRO Collaboration

M. Ambrosio[12], R. Antolini[7], G. Auriemma[14,a], R. Baker[11], A. Baldini[13], G. C. Barbarino[12], B. C. Barish[4], G. Battistoni[6,b], R. Bellotti[1], C. Bemporad[13], P. Bernardini[10], H. Bilokon[6], V. Bisi[16], C. Bloise[6], T. Bosio[7], C. Bower[8], S. Bussino[14], F. Cafagna[1], M. Calicchio[1], D. Campana[12], M. Carboni[6], M. Castellano[1], S. Cecchini[2,c], F. Cei[13,d], V. Chiarella[6], A. Corona[14], S. Coutu[11], L. De Benedictis[1], G. De Cataldo[1], H. Dekhissi[2,e], C. De Marzo[1], I. De Mitri[9], M. De Vincenzi[14,f], A. Di Credico[7], O. Erriquez[1], R. Fantini[2], C. Favuzzi[1], C. Forti[6], P. Fusco[1], G. Giacomelli[2], G. Giannini[13,g], N. Giglietto[1], M. Goretti[14], M. Grassi[13], P. Green[m], A. Grillo[7], F. Guarino[12], P. Guarnaccia[1], C. Gustavino[7], A. Habig[8], K. Hanson[11], A. Hawthorne[8], R. Heinz[8], J. T. Hong[3], E. Iarocci[6,h], E. Katsavounidis[4], E. Kearns[3], S. Kyriazopoulou[4], E. Lamanna[14], C. Lane[5], D. S. Levin[11], P. Lipari[14], G. Liu[4], R. Liu[4], N. P. Longley[n], M. J. Longo[11], G. Ludlam[3], F. Maaroufi[2,e], G. Mancarella[10], G. Mandrioli[2], A. Margiotta-Neri[2], A. Marini[6], D. Martello[10], A. Marzari-Chiesa[16], M. N. Mazziotta[1], D. G. Michael[4], S. Mikheyev[7,i], L. Miller[8], P. Monacelli[9], T. Montaruli[1], M. Monteno[16], S. Mufson[8], J. Musser[8], D. Nicoló[13,d], R. Nolty[4], C. Okada[3], C. Orth[3], G. Osteria[12], S. Paganini2, O. Palamara[10], S. Parlati[7], V. Patera[6,h], L. Patrizii[2], R. Pazzi[13], C. W. Peck[4], S. Petrera[10], N. D. Pignatano[4], P. Pistilli[10], V. Popa[2,l], A. Rainó[1], J. Reynoldson[7], F. Ronga[6], U. Rubizzo[2,c], A. Sanzgiri[15], F. Sartogo[14], C. Satriano[14,a], L. Satta[6,h], E. Scapparone[7], K. Scholberg[4], A. Sciubba[6,h], P. Serra-Lugaresi[2], M. Severi[14], M. Sitta[16], P. Spinelli[1], M. Spinetti[6], M. Spurio[2], R. Steinberg[5], J. L. Stone[3], L.R. Sulak[3], A. Surdo[10], G. Tarlé[11], V. Togo[2], V. Valente[6], C. W. Walter[4] and R. Webb[15]

1. Dipartimento di Fisica dell'Università di Bari and INFN, 70126 Bari, Italy
2. Dipartimento di Fisica dell'Università di Bologna and INFN, 40126 Bologna, Italy
3. Physics Department, Boston University, Boston, MA 02215, USA
4. California Institute of Technology, Pasadena, CA 91125, USA
5. Department of Physics, Drexel University, Philadelphia, PA 19104, USA
6. Laboratori Nazionali di Frascati dell'INFN, 00044 Frascati (Roma), Italy
7. Laboratori Nazionali del Gran Sasso dell'INFN, 67010 Assergi (L'Aquila), Italy
8. Depts. of Physics and of Astronomy, Indiana University, Bloomington, IN 47405, USA
9. Dipartimento di Fisica dell'Università dell'Aquila and INFN, 67100 L'Aquila, Italy
10. Dipartimento di Fisica dell'Università di Lecce and INFN, 73100 Lecce, Italy
11. Department of Physics, University of Michigan, Ann Arbor, MI 48109, USA
12. Dipartimento di Fisica dell'Università di Napoli and INFN, 80125 Napoli, Italy
13. Dipartimento di Fisica dell'Università di Pisa and INFN, 56010 Pisa, Italy
14. Dipartimento di Fisica dell'Università di Roma "La Sapienza" and INFN, 00185 Roma, Italy
15. Physics Department, Texas A&M University, College Station, TX 77843, USA
16. Dipartimento di Fisica Sperimentale dell'Università di Torino and INFN, 10125 Torino, Italy
a Also Università della Basilicata, 85100 Potenza, Italy
b Also INFN Milano, 20133 Milano, Italy
c Also Istituto TESRE/CNR, 40129 Bologna, Italy
d Also Scuola Normale Superiore di Pisa, 56010 Pisa, Italy
e Also Faculty of Sciences, University Mohamed I, B.P. 424 Oujda, Morocco
f Also Dipartimento di Fisica, Università di Roma Tre, Roma, Italy
g Also Università di Trieste and INFN, 34100 Trieste, Italy
h Also Dipartimento di Energetica, Università di Roma, 00185 Roma, Italy
i Also Institute for Nuclear Research, Russian Academy of Science, 117312 Moscow, Russia
l Also Institute for Atomic Physics, 76900 Bucharest, Romania
m Sandia National Laboratory, Albuquerque, NM 87185, USA
n Swarthmore College, Swarthmore, PA 19081, USA

Abstract

Using 5.33×10^6 single muons collected in 1.46×10^4 live hours by MACRO during the period 1991-1994, we have searched for a correlation between variations in the underground muon rate, N_μ, and seasonal temperature variations in the atmosphere. These correlations are found to be present with high statistical significance. Analysis of the relatively complete December 1992-December 1994 subset of the data yields a value for the temperature coefficient, $\alpha_T = (T/N_\mu)(\partial N_\mu/\partial T) = 0.83 \pm 0.13$. Analysis of the total data set gives consistent results.

We have compared this result with the hypothesis that the muons observed in MACRO come from pion decays alone. Although our result is consistent with the "pion only" hypothesis, a discussion of the sensitivity of our data sample to the kaon component of the cascades leading to observed muons underground will also be presented.

1 Introduction

Underground muons originate primarily from the decay of mesons produced in high energy interactions between primary cosmic ray particles and atmospheric nuclei [1]. As shown decades ago [2-4], fluctuations in atmospheric temperature lead to variations in the muon intensity observed at ground level and underground. Above ground, these variations have been relatively well-studied [5, and references therein]. However, there have been relatively few experimental measurements of these effects underground, and those that have been made have not always been in agreement with theory [6-15].

MACRO is a large acceptance, deep underground detector located in the Gran Sasso underground laboratory in Italy. Its large collecting area and great depth make it a powerful tool for the investigation of atmospheric temperature effects on the underground muon rate. MACRO's large collecting area results in large number statistics. Its great depth translates into a greater fractional difference in the muon rate for a given temperature change when compared with shallower detectors. There are two reasons for this. At great depths muons tend to come from higher energy pion and kaon parents; these higher energy parents are more likely to interact in the atmosphere than decay. Since the temperature effect we seek is due to differential variations in the atmospheric interaction rate of the parent mesons, large depths tend to maximize the effect. Further, the muons reaching MACRO are sufficiently energetic that they are unlikely to decay to electrons, again increasing the magnitude of the effect.

In the work reported here, muon data obtained during 1991-1994 have been analyzed for systematic variations resulting from seasonal variations in atmospheric conditions.

2 Meteorological Effects on the Muon Rate Observed Underground

2.1 Correlation of Intensity Variations with Atmospheric Temperature

The dependence of muon intensity variations on the atmospheric temperature is often expressed phenomenologically as [2]:

$$\frac{\Delta I_\mu}{I_\mu^0} = \int_0^\infty dX\, \alpha(X)\, \frac{\Delta T(X)}{T(X)}. \tag{1}$$

In this equation, $I_\mu^0 = I_\mu(T_0, > E_{th})$ is the differential muon intensity integrated from the detector threshold, $E_{th}(\approx 1.3$ TeV for MACRO), to infinity assuming the atmosphere is isothermal at temperature T_0, and ΔI_μ are fluctuations about I_μ; $\alpha(X)$ is

the "temperature coefficient" that relates fluctuations in the atmospheric temperature at depth X, $\Delta T(X)/T(X)$, to the fluctuations in the integral muon intensity; and the integral extends over atmospheric depth from the altitude of muon production to the ground. (For a detailed discussion of this relation, see the appendix.) For typical primary interactions at $\sim$ 20 km, the upper limit of the integral can be extended to infinity [1]. As described by Barrett *et al.* [2], the temperature coefficient for a deep detector like MACRO is dominated by a positive correlation between the underground muon intensity and the atmospheric temperature. As the atmospheric temperature increases, the density of the air decreases and fractionally more pions/kaons decay to muons before interacting. Although the magnitude of α can be reduced somewhat by the decay of surviving muons to electrons, this effect is unimportant for MACRO where the threshold energy for muons at the surface to be detected underground is high.

There is also a variation of the intensity with pressure that was extensively explored by Sagisaka [5]. Detailed computations, however, show that fluctuations in the intensity due to pressure variations are at least an order of magnitude smaller than those due to temperature variations for deep underground detectors and are thus ignored in this analysis.

We now cast Eq.(1) in a form suitable for the experimental determination of α. We write the integral muon intensity in the usual way,

$$I_\mu = \frac{N_i/t_i}{\epsilon A_{eff}\Omega},$$

where N_i are the single muons observed during live time t_i, ϵ is the efficiency for muon track reconstruction, A_{eff} is the detector effective area, and Ω is the total solid angle viewed by the detector. For data-taking over periods of weeks to months, A_{eff} and Ω are constant. In addition, several investigations have shown that the magnitude of the fluctuations in the muon rate due to atmospheric temperature variations are small, of the order of a few percent. For this reason the data set used in this investigation has been very carefully defined to exclude effects that could mask the atmospheric variations we are searching for. We require track geometries such that the probability of track detection is known *a priori* to be 100%. A data set selected in this way has $\epsilon = 1$ and requires no corrections for efficiency. The fluctuations in the integral muon intensity are then

$$\begin{aligned} \Delta I_\mu/I_\mu &= \left[\frac{\Delta N_i/t_i}{\epsilon A_{eff}\Omega}\right] \Big/ \left[\frac{N_i/t_i}{\epsilon A_{eff}\Omega}\right] = \left[\Delta N_i/t_i\right] \Big/ \left[N_i/t_i\right] \\ &= \Delta R_\mu/R_\mu \approx (R_\mu - \bar{R}_\mu)/\bar{R}_\mu, \end{aligned} \tag{2}$$

where $R_\mu = N_i/t_i$ is the muon rate observed underground during live time t_i and $\bar{R}_\mu = \sum N_i / \sum t_i$ is the average muon rate over the total data-taking period $\sum t_i$.

As shown in the Appendix, we can simplify the integral in Eq.(1) by introducing the "effective temperature", T_{eff} [2]. With this approximation, the integral in Eq.(1) becomes

$$\begin{aligned} \int_0^\infty dX \alpha(X) \frac{\Delta T(X)}{T(X)} &= \alpha_T \frac{\Delta T_{eff}}{T_{eff}} \\ &\approx \alpha_T (T_{eff} - \bar{T}_{eff})/\bar{T}_{eff}, \end{aligned} \tag{3}$$

where α_T is the depth-weighted temperature coefficient and $\bar{T}_{eff}$ is the average effective temperature during the data-taking period, $\sum t_i$. With these approximations, Eq.(1) can be written

$$\Delta R_\mu / \bar{R}_\mu = \alpha_T \, \Delta T_{eff} / \bar{T}_{eff}, \tag{4}$$

where $\Delta T_{eff} = T_{eff} - \bar{T}_{eff}$. This is the expression we have used to study the seasonal variations in the underground muon rate at MACRO. This is the experimental form of Eq.(A.11).

2.2 The Effective Temperature

The effective temperature, as defined in Eq.(A.8), is difficult to evaluate in general. However, for the case in which the observed muons come from pion decay alone, a simple expression for T_{eff} can be derived. In this case,

$$\begin{aligned} T_{eff} &= \frac{\int T(X)\, dX/X \, [\exp(-X/\Lambda_\pi) - \exp(-X/\Lambda_N)]}{\int dX/X \, [\exp(-X/\Lambda_\pi) - \exp(-X/\Lambda_N)]} \\ &\approx \frac{\sum_i [T(X_i)/X_i] \, [\exp(-X_i/\Lambda_\pi) - \exp(-X_i/\Lambda_N)]}{\sum_i (1/X_i) \, [\exp(-X_i/\Lambda_\pi) - \exp(-X_i/\Lambda_N)]}, \end{aligned} \tag{5}$$

where $\Lambda_\pi = 160$ gm/cm^2 is the atmospheric attenuation length for pions, $\Lambda_N = 120$ gm/cm^2 is the atmospheric attenuation length for nucleons, and the integral is to the top of the atmosphere. We have approximated the integral by a sum to account for the fact that temperature measurements are only available at discrete levels X_i. According to Barrett *et al.* [2], this form for the effective temperature includes the principal effects of the temperature distribution in the atmosphere by assigning weights to different atmospheric levels according to the relative importance of this level in the production of the muons observed underground. By making this choice for T_{eff}, we are testing the hypothesis that the muons observed underground come from pion decay alone. To the extent that we see significant deviations from this model, we would conclude that kaon decay must be explicitly included in the analysis.

3 Data Analyzed

3.1 Muon Data Sample

For this investigation, data have been collected with the lower structure of MACRO, which consists of six nearly identical units called supermodules, each of dimension 12.6m × 12m × 4.8m. (For a complete description of the detector, see [16].) Each supermodule is further divided into two identical modules. Each module consists of 10 horizontal planes of streamer tubes, 12m × 6m. The 8 innermost planes are separated by seven layers of 60 gm/cm^2 absorber of low activity Gran Sasso rock. The two outermost planes are each separated from the next nearest streamer tube plane by a 25 cm layer of liquid scintillator. The lateral walls consist of stacked tanks of liquid scintillator, 25 cm thick, sandwiched between six vertical streamer tubes planes. All streamer tube wires are read out, providing the X coordinate on the horizontal planes and the Z coordinate on the vertical planes. On the horizontal planes the second coordinate, D, is obtained by reading the pulses induced on horizontal aluminum strips oriented 26.5^0 with respect to the streamer tube axis. These strips allow stereoscopic reconstruction. Typically, the efficiency of the wires is $\sim$ 95% to record a hit for a throughgoing particle; the efficiency of the strips is $\sim$ 90%. In the track reconstruction algorithm, a search is first made for a set of aligned points. A linear fit to these selected points is then performed, and the track parameters are calculated. A muon track is reconstructed if hits are recorded on at least four horizontal planes, both in the wire and strip views. The probability that a muon crossing 10 horizontal planes of streamer tubes will have a reconstructed track is better than 99%.

We first applied a run cut to ensure that the streamer tubes were operating efficiently. Within a run we then applied a geometrical cut: individual events were required to cross all 10 horizontal streamer tube tracking planes; in practice we applied this cut by accepting those tracks pointing through the top and bottom planes of a single module. In addition, only single track muon events were analyzed to avoid any tracking ambiguities. By carefully investigating events that triggered the top and bottom scintillator planes of a single module we have found that virtually 100% of events with this geometry resulted in a reconstructed track. Therefore, by selecting events with this geometry, we have defined a data set with $\epsilon = 1$ that requires no corrections for efficiency.

Monte Carlo computations, like those described in [17], show that the acceptance for the lower six supermodules for events crossing the top and bottom planes of the entire detector in a single module is $A_{eff} \times \Omega \simeq 901.8$ m$^2 \times 1.90\pi$ sr $\simeq 5,400$ m^2 sr.

Data were collected during a 4 year period starting in January 1991, when the streamer tubes in all six supermodules were turned on, and ending in December 1994. The data used in this analysis were divided into two sets based on the relative performance of the streamer tube system: the first set is comprised of runs from January 1991-November 1992 when the streamer tube system had yet to be opti-

mized (data set 1); the second, higher quality data set includes runs from December 1992-December 1994 when MACRO operated in a mode optimized for data-taking (data set 2).

The specific data cuts used in this analysis are listed below in the order in which they were applied. Given in parentheses are the percentages of events lost due that cut for data set 1 and data set 2, respectively, based on the number of events surviving the previous cuts.

Event cuts:
(1) Events were required to have a single track in both the strip and wire views (4.5%, 4.5%). (2) Events were required to geometrically cross all 10 streamer tube planes in a single module (53%, 53%).

The run cuts were made in a manner that reflects the way in which MACRO data are read out. In the MACRO data acquisition system, the data from two adjacent supermodules (4 modules) are read out by individual μVAX computers. Except for run cut #1, run cuts were consequently made on a μVAX-by-μVAX basis to minimize the exclusion of good data from the analysis.
Run cuts:
(1) Runs were cut when all six supermodules were not in acquisition (37.6%, 12.1%). (2) Runs with low wire efficiency and/or low strip efficiency were cut. In particular, runs were cut when the average number of wire hits read out was less than 9.0/10 or for which the average number of strip hits read out was less than 8.0/10. (27.3%, 6.8%). Tests verify that for all runs passing these cuts, 100% of the 10 plane crossers within one module had tracks reconstructed. The runs excluded due to this cut are shown shaded in Figure 1 where the average number of wires read out and the average number of strips read out for the two data taking periods have been plotted. For the primary data set, data set 2, this cut is not extremely restrictive. For data set 1, the same cut was adopted as a measure of run quality. (3) Runs with rates that deviate by more than 3σ from the mean were cut (1.0%, 2.0%). (4) Several runs were cut due to problems recorded by run coordinator or the shiftworkers in the online log books (1.3%, 4.5%)

In Table 1 we list for each data set the effect of the cuts on the number of muons and the effective live time. This table clearly shows that the overall data quality is significantly higher in data set 2. Given along the bottom row are the totals; the data sample comprises a grand total of 5.33×10^6 muons and a total live time of 1.46×10^4 hours.

In Figure 2 we show $\Delta R_\mu = (R_\mu - \bar{R}_\mu)$ (muons/hr), by month from June 1991-December 1994. R_μ is the monthly average of the rate and $\bar{R}_\mu = 364.8$ muons/hr is the average rate for December 1992-December 1994. The errors on ΔR_μ in Figure 2 are the quadratic sum of the statistical error in the monthly rate, $\sqrt{\sum N}/t$, and the error in the mean, $\bar{R}_\mu$. This figure (and Table 1) suggests that the data for 1991 and 1992 are incomplete. Further, the months for which the complete MACRO was in

acquisition were the summer months when rates are expected to be systematically higher than the yearly mean (the seasonal effect we seek). Consequently, if the 1991-1992 data were used in the computation of $\bar{R}_\mu$, the mean would be biased high. For this reason, we have only used the relatively complete data sample from December 1992 through 1994 (data set 2) in the computation of $\bar{R}_\mu$.

Figure 2 clearly shows that there are seasonal variations in the muon rate of magnitude a few percent, as expected.

3.2 Temperature Data

The temperature data were provided by the Ispettorato Telecomunicazioni ed Assistenza Volo dell'Aeronautica Italiana. For the years 1991-1993, the data were obtained at 8 atmospheric depths (700 gm/cm^2, 500 gm/cm^2, 300 gm/cm^2, 150 gm/cm^2, 70 gm/cm^2, 45 gm/cm^2, 35 gm/cm^2, 25 gm/cm^2) four times daily: 0^h, 6^h, 12^h, and 18^h. In 1994, there were only two flights per day, at 11^h and 23^h. The depth sampling during these flights was much finer, however. To be consistent with the previous years we only used data at depths $\leq$ 700 gm/cm^2.

We computed T_{eff} using Eq.(5) with the data returned from each flight. For each month, we computed the mean of the distribution of that month's effective temperatures. In Figure 3 we show the monthly fluctuations in this mean, $\Delta T_{eff} = (T_{eff} - \bar{T}_{eff})$, where T_{eff} is the mean effective temperature for the month, and $\bar{T}_{eff} = 217.8\,\mathrm{K}$ the average mean effective temperature computed for the complete data set. The monthly error on ΔT_{eff} is taken equal to the standard deviation of the T_{eff} distribution for that month. The larger errors for 1994 are likely due to poorer sampling during the day.

4 Results

4.1 Correlation of the Fluctuations

In Figure 4 we superpose the percentage fluctuations in the effective temperature for December 1992-December 1994 onto the percentage fluctuations in the muon rate. Our analysis concentrates on the data set from December 1992-1994 since these data are the most complete and MACRO was running in an optimized data-taking mode.

There is a clear correlation present between the systematic variations in the underground muon rate and the variations in the effective temperature. To quantify the significance of the correlation, we have computed both the correlation coefficient and the chance probability that the variations in the muon rate and the effective temperature are uncorrelated (null hypothesis). The results of these computations are given in Table 2. This table clearly demonstrates that the variations in the muon rate and the effective temperature are highly correlated.

Finally, we have repeated the analysis for the combined data for 1991-1994. In this analysis, we have averaged the data for a given month over all four years. The

four-year monthly average muon rates we computed are shown in Figure 5. As before, we have only used data from December 1992 through 1994 in the determination of $\bar{R}_\mu$ to avoid bias. Superposed are the monthly weighted means of the temperature variations. The results of the correlation analysis are given in Table 2. These variations are also highly correlated.

4.2 Experimental Determination of α_T

In our determination of α_T, we first used the December 1992-December 1994 data set. The computation proceeds by fitting the regression line of the form shown in Eq.(4) using the algorithm in **Numerical Recipes** [18] that includes errors in both variables, $\Delta R_\mu/\bar{R}_\mu$ and $\Delta T_{eff}/\bar{T}_{eff}$. As discussed in this reference, when there are errors in both variables, there is no simple least-squares alternative to their procedure. In Table 2 we give the result of this computation, $\alpha_T = 0.83 \pm 0.13$; repeating the analysis for the total data set, we find $\alpha_T = 0.98 \pm 0.12$. The formal error for the primary data set is larger primarily due to the larger errors in the 1994 temperatures. This table also lists the value of $\alpha_T/\bar{T}_{eff} \times 100$ (%/K), the units in which α_T is often expressed.

4.3 The Predicted α_T

We have computed the expected value of α_T for MACRO under the assumption that the muons come from pion decay alone. To the extent that the experimental result differs from this value, we can conclude kaons must be included in the analysis. For comparison with our experimental value, we compute the average of Eq.(A.18),

$$< \alpha_T >_\pi = \langle \, 1 \Big/ \left[1 + \frac{\gamma}{(\gamma+1)} \times \frac{\epsilon_\pi}{1.1\, E_{th} \cos\theta} \right] \rangle. \qquad (6)$$

Here $E_{th} \cos\theta$ is the product of the threshold energy, E_{th}, and the cosine of the zenith angle, θ, for events in the muon sample. In addition, γ is the spectral index of the muon intensity, which for MACRO is $\gamma = 1.78$ [19]. We have written a Monte Carlo program to calculate the expected value for $< \alpha_T >_\pi$.

For this computation, we first chose a muon energy, E_μ, and zenith angle, θ, from the inclusive muon intensity, Eq.(A.1), and a random azimuthal angle, ϕ. For the zenith and azimuthal angles selected, we found the rock depth, $D(\theta, \phi)$, from the known rock distribution above MACRO. Using the MACRO survival probability tables, we then randomly selected whether this muon reaches MACRO. If the muon successfully reaches the detector, we tested whether this muon would successfully cross 10 planes in a single module by placing it at a random position on the top of the detector and checking whether its momentum vector points through the bottom face of the module directly below its starting point. Using successful 10 plane crossers we computed the average $< \alpha_T >_\pi$.

We simulated the systematic effect of excluding multiple muons from the data analysis by using the parameterizations of coincident multiple muons described in Gaisser [1], although we expect the effect of multiple muons on the data sample to be small. Multiple muons are relatively rare and should have only a small impact on the analysis. In addition, multiple muons come on average from primaries of higher energy than single muons. As seen in Figure 6, where $< \alpha_T >_\pi$ is plotted for MACRO (as described below), the curve for $< \alpha_T >_\pi$ flattens out at depths below MACRO. Since muons that survive to lower depths typically come from higher energy primaries, this curve also shows the effect of including a greater fraction of high energy primaries on the computation of $< \alpha_T >_\pi$. This figure also suggests that the effect of including multiple muons in the analysis should be minimal.

In this simulation, we only investigated the effect of double muons; if double muons have a negligible effect, we expect that the much rarer higher multiplicity bundles would have an even smaller impact on our data analysis. For each successful 10 plane crosser of energy E_μ at the surface, we selected a primary energy out of the 'muon response function' appropriate for muons with $> E_\mu$. As discussed by Gaisser [1], the muon response function is the integral of the distribution of cosmic rays with primary energies, E_0, that produce muons at the surface with energies $> E_\mu$, $dN_\mu(> E_\mu)/dE_0$. In particular, we used the muon response function for muons > 139 GeV, as computed by Gaisser [20], which we extrapolated to the appropriate $> E_\mu$ assuming that the response function scales with energy [21]. This procedure is an approximation that we adopt in lieu of detailed computations of atmospheric cascades to determine the primary energy distribution for all appropriate values of E_μ. The effect of this approximation is to overestimate the parent nucleon energy, thereby overestimating the fraction of muon bundles excluded by our data analysis. Using the selected parent energy, we then chose a primary nucleus out of distributions obtained by combining the proton and helium spectra from JACEE [23] and the heavier mass group spectra from CRN [24]. These choices were motivated by the conclusions of the MACRO multiple muon studies [22] which find that these mass spectra provide the most consistent fit to the multiple muon data. Once the energy and mass of the primary were chosen, we used the parameterizations in Gaisser [1], which are based on the work of Forti *et al.* [25], to select a multiplicity for the event. Those events with multiplicity greater than 2 were excluded from the computation; those events with multiplicity 1 were counted in the computation. For events with multiplicity 2, we continued by selecting a separation distance from the lateral spread distribution in Gaisser [1]. We combined the selected lateral distance and a random azimuth with respect to the first muon to determine a trajectory for the second muon, and tested whether the second muon crossed any face of MACRO. If the second muon hit MACRO, the event was excluded; if it missed, the event was counted. These computations show that the exclusion of multiple muons changes $< \alpha_T >$ by $\sim 0.1\%$. The effect of systematics on these Monte Carlo computations, for example the extrapolation of the muon response function to higher energies or the CRN/JACEE spectra for the primaries, is hard to quantify. It is unlikely, however,

that these systematics could alter the result by more than an order of magnitude. We believe therefore that these computations demonstrate that the exclusion of multiple muons has a negligible effect on the data analysis presented here.

The results of the calculation show $< \alpha_T >_\pi = 0.96$. When kaons are included in the scaling limit, $< \alpha_T >= 0.90$, a 6% difference from the pion-only value. Further, it needs to be stressed that this is a 6% variation on $\sim$ 4% peak-to-peak fluctuations. The simulation shows that excluding double muons from the analysis has virtually no effect on the results; we extrapolate from this result that excluding all multiples has no effect on the results. Based on these Monte Carlo calculations, we have also found that the fraction of muons coming from pion decays in our data sample to be 0.77, and the fraction from kaon decays to be 0.23.

Volkova and Zatseypin [26] who made an extended and detailed computation of the temperature coefficients for all possible mechanisms of high energy muon generation found results similar to those presented here.

4.4 Comparison with Other Experiments

In Figure 6 we show the MACRO result compared with other measurements taken from the literature. The theoretical curve has been computed for muons from pion decay alone, corrected at low energies for muon decay to electrons according to Barrett *et al.* [2]. Again, Eq.(6) was used for the Monte Carlo computation of $< \alpha_T >_\pi$. For each depth in the grid, we chose a muon energy, E_μ, and zenith angle, $\theta < 72°$, from the inclusive muon intensity, Eq.(A.1), and a random azimuthal angle, ϕ. We then tested whether the selected muon had sufficient energy to reach a perfect detector at this depth, assuming a flat overburden. The average was computed for 10,000 successful muons. No experiment-specific data cuts were made, as in the MACRO-specific computation of $< \alpha_T >_\pi$ described above. At shallow depths, $< \alpha_T >_\pi$ is small because the threshold energy is so low that interactions are unimportant in the cascades. At large depths, $< \alpha_T >_\pi$ increases slowly because the cascades are now totally dominated by collisions. As seen in Figure 6, the MACRO result is consistent with this hypothesis. References to the other experimental values are listed in the figure caption. Typically, measurements are reported as α_T/T_0 in units %/°K. We have chosen to compare experimental results to α_T, the experimentally determined quantity. For comparison, we list $\alpha_T/\bar{T}_{eff}$ in Table 2. For experiments not reporting T_0, we chose $T_0 = 223$ °K, as given in Barrett *et al.* [2]. The results from Sherman [13], Utah [9] and Poatina [8] deviate significantly from the theoretical curve; these descrepancies are likely due to their choice of a value of T_0 from lower altitudes, 100-300 mb.

5 Conclusions

We have analyzed 5.33×10^6 single muons obtained over 1.46×10^4 live hours during 1991-1994 in a search for correlations between variations in the underground muon rate seen in MACRO and systematic seasonal variations in atmospheric temperature. We find that these correlations are clearly present. Computation of the correlation coefficient quantifies that the correlation is extremely unlikely to be due to random chance.

The MACRO results are consistent with measurements made at similar depths by other experiments and with the theoretical expectation for muons coming from pion decay alone.

The experimental determination of the temperature coefficient, $\alpha_T = 0.83 \pm 0.13$, allows us to assess the sensitivity of our measurement to the addition of kaons into our flux models. If we define as the "null hypothesis" the case that all muons detected in our apparatus result from pion decays alone, our results are not inconsistent with this hypothesis. However, the introduction of the kaon contribution into these calculations gives slightly better agreement between our data and the expected value of α_T. The lack of sensitivity to the kaon component is not due to lack of statistics, but rather the large uncertainty in the experimental temperature coefficient that comes mostly from the errors in T_{eff}. This approximation to the true run of temperature with depth is unlikely to accurately quantify α with the precision necessary to see an effect of $< 1\%$ in the muon rate (a 6% change in a 4% fluctuation).

6 Acknowledgements

We gratefully acknowledge the support of the director and of the staff of the Laboratori Nazionali del Gran Sasso and the invaluable assistance of the technical staff of the Institutions participating in the experiment. We thank the Istituto Nazionale di Fisica Nucleare (INFN), the U.S. Department of Energy and the U.S. National Science Foundation for their generous support of the MACRO experiment. We thank INFN for providing fellowships and grants (FAI) for non Italian citizens.

We also wish to thank the Ispettorato Telecomunicazioni ed Assistenza Volo dell'Aeronautica Italiana for kindly providing the temperature data.

References

[1] Gaisser, T. **Cosmic Rays and Particle Physics** (Cambridge University Press: Cambridge) (1990).

[2] Barrett, P.H., *et al.*, *Rev.Mod.Phys.*, **24** (1952) 133.

[3] Duperier, A., *Proc.Phys.Soc.*, **A62** (1949) 684; *J.Atmos.Terr.Phys.*, **1** (1951) 296.

[4] Trefall, H., *Proc.Phys.Soc.*, **A68** (1955) 625.

[5] Sagisaka, S., *Il Nuovo Cim.*, **9C** (1986) 809.

[6] Barrett, P.H., *et al.*, *Phys.Rev.*, **95** (1954) 1573.

[7] Cini Castagnoli, G., and Dodero, M.A., *Il Nuovo Cim.*, **51B** (1967) 525. (Torino)

[8] Humble, J.E., *et al.*, **Proc. 16th ICRC** (Kyoto), 4 (1979) 258. (Poatina)

[9] Cutler D.J., *et al.*, **Proc. 17th ICRC** (Paris) 4 (1981) 290. (Utah)

[10] Andreyev, Yu.M., *et al.*, **Proc. 20th ICRC** (Moscow) **3** (1987) 270; Andreyev, Yu.M., *et al.*, **Proc. 21st ICRC** (Adelaide) **7** (1990) 88; Andreyev, Yu.M., **Proc. 22nd ICRC (Dublin) 3** (1991) 693. (Baksan)

[11] Murakata, K., Yasue, S., and Mori, S., *J.Geomag.Geoelec.*, **40** (1988) 1023. (Matsushiro)

[12] Oyama, Y., *et al.*, **Proc. 22nd ICRC (Dublin) 3** (1991) 671. (Kamioka)

[13] Sherman, N., *Phys.Rev.*, **93** (1954) 208.

[14] Fenton, A.G., Jacklyn, R.M., and Taylor, R.B., *Il Nuovo Cimento*, **22B** (1961) 285. (Hobart)

[15] Dorman, L.I., **Cosmic Ray Variations**, State Publishing House for Technical and Theoretical Literature, Moscow, translation by US Air Force Tech. Doc. Liason Office (1958).

[16] The MACRO Collaboration, in preparation.

[17] The MACRO Collaboration, *Astrophys.J.*,**412** (1993) 301.

[18] Press, W.H., Teukolsky, S.A., Vettering, W.T., and Flannery, B.P. **Numerical Recipes in Fortran**, 2nd edition (Cambridge University Press: Cambridge) (1992)

[19] The MACRO Collaboration, *Physical Rev.D*, **52** (1995) 3793.

[20] Gaisser, T.K. *J.G.R.*, **79** (1974) 2281.

[21] Gaisser, T.K., private communication.

[22] The MACRO Collaboration, *Physics Lett.B*, **337** (1994) 376.

[23] The JACEE Collaboration: Burnett *et al.*, *Astrophys.J.Lett.*, **349** (1990) L25.

[24] The CRN Collaboration: Muller, D., *et al.*, *Astrophys.J.*, **374** (1991) 356.

[25] Forti, C. Thesis: University of Rome, "La Sapienza" (1988).

[26] Volkova, L.V., and Zatsepin, G.T., *Soviet J.Nucl.Phys.*, **12** (1971) 191.

A Dependence of Intensity on Atmospheric Temperature

As described in Gaisser [1], the differential intensity of muons as a function of energy at the surface, dI_μ/dE_μ, is given by the integral of the production spectrum of muons, P_μ, over atmospheric depth, X (gm/cm^2),

$$\begin{aligned}\frac{dI_\mu}{dE_\mu} &= \int_0^\infty dX P_\mu(X, E_\mu) \\ &= 0.14 \times E_\mu^{-(\gamma+1)} \times \left(\frac{1}{1 + \frac{1.1 E_\mu \cos\theta}{\epsilon_\pi}} + \frac{0.054}{1 + \frac{1.1 E_\mu \cos\theta}{\epsilon_K}} \right). \end{aligned} \tag{A.1}$$

Here E_μ is the muon energy; θ is the muon zenith angle; $\gamma = 1.78$ is the spectral index for the muons observed by MACRO [19]; and $\epsilon_\pi = 115$ GeV and $\epsilon_K = 850$ GeV are the pion critical energy and the kaon critical energy, respectively. This expression, which interpolates between low and high energy approximations, matches well the differential intensity at the depth of MACRO. The constants in this expression have been obtained from experimental data on cross sections and branching ratios. In the present analysis we are chiefly interested in the integral spectrum,

$$I_\mu(> E_{th}) = \int_{E_{th}}^\infty dE_\mu \frac{dI_\mu}{dE_\mu}, \tag{A.2}$$

where

$$E_{th} = E_{th}(\theta, \phi) = 0.53\,\text{TeV}\,(e^{0.4D} - 1) \tag{A.3}$$

is the muon energy threshold for reaching MACRO from direction (θ, ϕ) through rock depth $D = D(\theta, \phi)$ in kilometers of water equivalent. In analogy with Barrett *et al.* [2], a fair approximation to the integral in Eq.(A.2) is given by

$$I_\mu \approx B \times E_{th}^{-\gamma} \times \left[\frac{1}{\gamma + \frac{(\gamma+1)1.1 E_{th} \cos\theta}{\epsilon_\pi}} + \frac{0.054}{\gamma + \frac{(\gamma+1)1.1 E_{th} \cos\theta}{\epsilon_K}} \right]. \tag{A.4}$$

The sensitivity of the muon intensity to atmospheric temperature depends on the relative importance of interaction processes and decay processes in the atmospheric pion/kaon cascades that result in the muons seen underground. When interactions dominate, temperature variations translate directly into rate variations, making the muon rate sensitive to temperature. When decays dominate, the muon rate is less sensitive to the same temperature variations. The pion/kaon critical energy separates these two regimes; for pions, interactions dominate when

$$E_\mu \gg \epsilon_\pi = \frac{m_\pi c^2 H(T)}{c\tau_\pi},$$

where m_π and $c\tau_\pi$ are the mass and decay length of the pion; and $H(T) = RT/Mg$ is the atmospheric scale height for an isothermal, exponential atmosphere. A similar expression holds for kaons. The temperature dependence of I_μ is contained in the critical energy functions ϵ_π and ϵ_K. To first approximation, most of the particle interactions occur in the first few interaction lengths, and $H(T) \approx H_0 = 6.4$ km [1].

To find the variation of the integral intensity with atmospheric temperature, T, first expand P_μ

$$\begin{aligned} P_\mu(X, E_\mu, T_0 + \Delta T) &= P_\mu(X, E_\mu, T_0) + (\partial P_\mu/\partial T)_{T_0} \Delta T(X) \\ &= P^0_\mu(X, E_\mu) + \eta^0(X, E_\mu)\Delta T(X), \end{aligned}$$

where the superscript "0" denotes the evaluation of the temperature sensitive functions at $T = T_0$. The variation of the integral muon intensity is then

$$\begin{aligned} I_\mu(> E_{th}, T_0 + \Delta T) &= \int_{E_{th}}^{\infty} dE_\mu \int_0^\infty dX [P^0_\mu(X, E_\mu) + \eta^0(X, E_\mu)\Delta T(X)] \\ &= I^0_\mu + \int_0^\infty dX\, \Delta T(X) \int_{E_{th}}^{\infty} dE_\mu\, \eta^0(X, E_\mu). \end{aligned} \tag{A.5}$$

where $I^0_\mu = I^0_\mu(> E_{th})$. By setting $\Delta I_\mu = I_\mu(T_0 + \Delta T) - I^0_\mu$, the dependence of muon intensity variations on the temperature in the atmosphere can now be expressed in the usual way [2, 5, 15]:

$$\frac{\Delta I_\mu}{I^0_\mu} = \int_0^\infty dX\, \alpha(X)\, \frac{\Delta T(X)}{T(X)}, \tag{A.6}$$

where the "temperature coefficient" is given by

$$\alpha(X) = \frac{T(X)}{I^0_\mu} \int_{E_{th}}^{\infty} dE_\mu\, \eta^0(X, E_\mu). \tag{A.7}$$

As it stands, it is difficult to determine the temperature coefficient experimentally because the temperature variations with atmospheric depth are not known. We now use an approach first described in Barrett *et al.* [2] to simplify the integral in Eq.(A.7). Define an "effective temperature", T_{eff}, such that

$$T_{eff} = \frac{\int_0^\infty dX\, T(X) \int_{E_{th}}^{\infty} dE_\mu\, \eta^0(X, E_\mu)}{\int_0^\infty dX \int_{E_{th}}^{\infty} dE_\mu\, \eta^0(X, E_\mu)}, \tag{A.8}$$

and the "effective temperature coefficient", α_T,

$$\alpha_T = \frac{T_{eff}}{I^0_\mu} \int_0^\infty dX \int_{E_{th}}^{\infty} dE_\mu\, \eta^0(X, E_\mu). \tag{A.9}$$

With these definitions,

$$\int_0^\infty dX\, \alpha(X)\, \frac{\Delta T(X)}{T(X)} \;=\; \alpha_T\, \frac{\Delta T_{eff}}{T_{eff}}, \tag{A.10}$$

where ΔT_{eff} is defined analogously to T_{eff}. Eq.(A.6) now becomes

$$\frac{\Delta I_\mu}{I_\mu^0} = \alpha_T\, \frac{\Delta T_{eff}}{T_{eff}}. \tag{A.11}$$

This is the primary equation used to study the effects of atmospheric temperature variations on the underground muon intensity.

The effective temperature, as defined in Eq.(A.8), is difficult to evaluate in general. However, for the case in which the muon spectrum can be approximated by the scaling limit solution, the computation of the effective temperature becomes much simpler. At MACRO's depth, this approximation holds for muon production from pion decay since $E_{th} \approx 1.3\,\mathrm{TeV} \gg \epsilon_\pi = 0.115\,\mathrm{TeV}$. However, the same approximation does not hold for kaons at MACRO's depth. For this reason, we first discuss the case for muon production from pion decay alone. At the end, we argue how this analysis can be extended to estimate the effect of kaons.

The X-dependence of the muon production spectrum in the scaling limit can be factored, $P_\mu(X, E_\mu, T) = h(X)\Pi(E_\mu, T)$ [1]. Assuming that the temperature dependence on X has only negligible effect on the factorization, then

$$\eta^0(X) = h(X)(\frac{\partial \Pi}{\partial T})_{T_0}, \tag{A.12}$$

and

$$T_{eff} = \frac{\int dX\, h(X)\, T(X)}{\int dX h(X)}. \tag{A.13}$$

The explicit expression for $h(X)$ in this limit is [1]:

$$h(X) = \frac{\Lambda}{X}\left[\exp\left(-X/\Lambda_\pi\right) - \exp\left(-X/\Lambda_N\right)\right]. \tag{A.14}$$

where $\Lambda = \Lambda_\pi\Lambda_N/(\Lambda_\pi - \Lambda_N)$, $\Lambda_\pi = 160$ gm/cm^2 is the atmospheric attenuation length for pions, and $\Lambda_N = 120$ gm/cm^2 is the atmospheric attenuation length for nucleons. For muon production from pions alone,

$$T_{eff} = \frac{\int T(X)\, dX/X\, \left[\exp\left(-X/\Lambda_\pi\right) - \exp\left(-X/\Lambda_N\right)\right]}{\int dX/X\, \left[\exp\left(-X/\Lambda_\pi\right) - \exp\left(-X/\Lambda_N\right)\right]}. \tag{A.15}$$

Substituting Eq.(A.12) into Eq.(A.9) gives

$$\begin{aligned} \alpha_T &= \frac{T_{eff}}{I_\mu^0} \times \int_0^\infty dX\, h(X) \times \int_{E_{th}}^\infty dE_\mu \frac{\partial \Pi}{\partial T} \\ &= \frac{T_{eff}}{I_\mu^0} \frac{\partial I_\mu}{\partial T}, \end{aligned} \tag{A.16}$$

which is the expected result. In practice, the value of T_{eff} is sufficiently close to T_0 in the upper atmosphere that only small changes are introduced into ϵ_π and ϵ_K when they are evaluated at T_{eff}. Barrett *et al.* [2] show that for a spectrum of the type described by Eq.(A.1),

$$\alpha_T = \frac{T}{I_\mu^0} \frac{\partial I_\mu}{\partial T} = -\frac{E_{th}}{I_\mu^0} \frac{\partial I_\mu}{\partial E_{th}} - \gamma, \tag{A.17}$$

which is the expression we used to compute the temperature coefficient. Evaluating this expression yields

$$(\alpha_T)_\pi = 1 \Big/ \left[1 + \frac{\gamma}{(\gamma+1)} \times \frac{\epsilon_\pi}{1.1\, E_{th} \cos\theta} \right] \tag{A.18}$$

for the temperature coefficient due to pion decay alone [2].

As discussed, we cannot extend this analysis to kaons at MACRO's depth. However, by extending the pion analysis above to kaons, we can estimate a lower limit to the magnitude of the effect. Since kaons have a much shorter decay length than pions, kaons have the effect of decreasing α_T even in the scaling limit approximation because a larger fraction of them decay rather than interact. For MACRO, α_T will be reduced further by the even greater fraction of kaons that decay. An estimate to the minimum effect that kaons can have on α_T comes from

$$\alpha_T = (\alpha_T)_\pi (1 - \zeta_K), \tag{A.19}$$

where ζ_K is the kaon correction to α_T in the scaling limit. It is simple to show that the changes in the weighting function for T_{eff} in Eq.(A.14) introduced by this approximation have a negligible effect on the value of T_{eff} since Λ_K differs from Λ_π by less than 15%. This means that we can test our determination of α_T using the T_{eff} in Eq.(A.15) against the hypothesis that $\zeta_K = 0$.

Figure Captions

Figure 1. Average number of wire planes and strip planes read out for events crossing 10 streamer tube planes in one MACRO module computed on a run-by-run basis for two data taking periods. The run cut was based on the December 1992-1994 data-taking period. The same run cut was imposed on the 1991-November 1994 data-taking period when the MACRO streamer tube system had not yet been fully optimized for data-taking.

Figure 2. Monthly variations in the mean muon rate, $\Delta R_\mu = (R_\mu - \bar{R}_\mu)$. R_μ is the mean monthly rate and $\bar{R}_\mu = 364.8$ muons/hr is the mean rate computed for the December 1992-1994 data set. The errors are dominated by statistical errors in the rates.

Figure 3. Monthly variations in the effective temperature, $\Delta T_{eff} = (T_{eff} - \bar{T}_{eff})$, where T_{eff} is the mean of the monthly effective temperature distribution and $\bar{T}_{eff} = 217.8$K is the mean effective temperature for the complete data set (1991-1994). The errors on the fluctuations are taken as the standard deviation in the T_{eff} distribution for that month.

Figure 4. The superposition of the mean monthly variations in the muon rate, $\Delta R_\mu / \bar{R}_\mu$ (%), and the mean monthly variations in the effective temperature, $\Delta T_{eff} / \bar{T}_{eff}$ (%)for the December 1992-1994 data set.

Figure 5. The superposition of the mean monthly variations in the muon rate, $\Delta R_\mu / \bar{R}_\mu$ (%), and the mean monthly variations in the effective temperature, $\Delta T_{eff} / \bar{T}_{eff}$ (%) for the averaged total data set, 1991-1994.

Figure 6. Experimental determination of the temperature coefficient α_T compared with the expected value for muon production from pion decay alone yas a function of depth. The value determined here is labelled MACRO; other experimental values include Baksan [10], Barrett 1 [2], Barrett 2 [6], Hobart [14], Kamioka [12], Matsushiro [11], Poatina [8], Sherman [13], Torino [7], and Utah [9]. The expected curve is from Eq.(A.17), with the energy-depth relation given by Eq.(A.3). The correction for muon decay to electrons is taken from Barrett *et al.*[2]. Typically, measurements are reported as α_T/T_0 in units %/°K. Here we compare experimental results to α_T, the experimentally determined quantity. For experiments not reporting T_0, we chose $T_0 = 223$ °K, as given in Barrett *et al.* [2].

Table 1: Data Sample – The Effect of Cuts on the Number of Selected Single Muons and Effective Live Times

Data Set		Total before Cuts	After Event Cuts	After Run Cuts
Jan 1991 - Nov 1992 (data set 1)	# muons:	1.11×10^7	4.71×10^6	1.55×10^6
	live time (h):	1.28×10^4	–	4.20×10^3
Dec 1992 - Dec 1994 (data set 2)	# muons:	1.19×10^7	5.06×10^6	3.78×10^6
	live time (h):	1.39×10^4	–	1.04×10^4
grand totals:	# muons:	2.30×10^7	9.77×10^6	5.33×10^6
	live time (h):	2.67×10^4	–	1.46×10^4

Table 2: Correlation Coefficient and Probability that Variations in the Muon Rate and Variations in the Effective Temperature are Uncorrelated (Null Hypothesis)

Data Set	Correlation Coefficient	Probability of Null Hypothesis	α_T	$\alpha_T/\bar{T}_{eff} \times 100^\dagger$ (%/K)
1993-1994	0.83	1.7×10^{-6}	0.83 ± 0.13	$0.38 \pm .057$
1991-1994	0.91	3.3×10^{-5}	0.98 ± 0.12	$0.45 \pm .055$

† the units in which α_T is usually expressed.

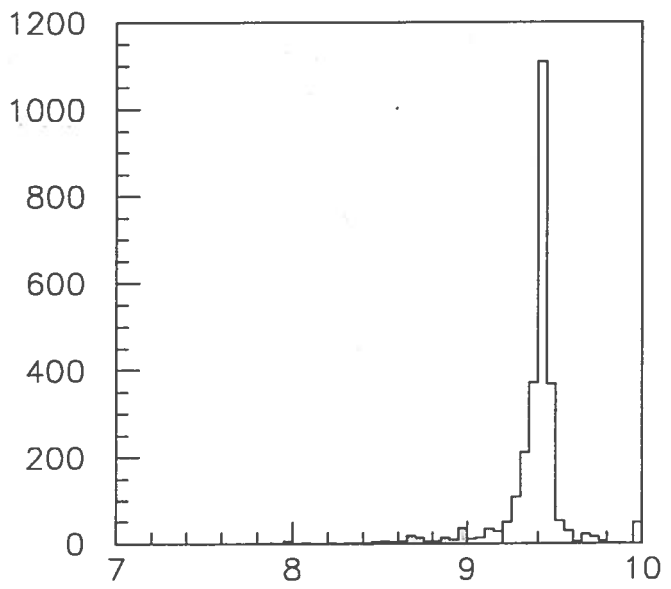

Avg. Wire Hits, Dec. 1992 – Dec. 1994

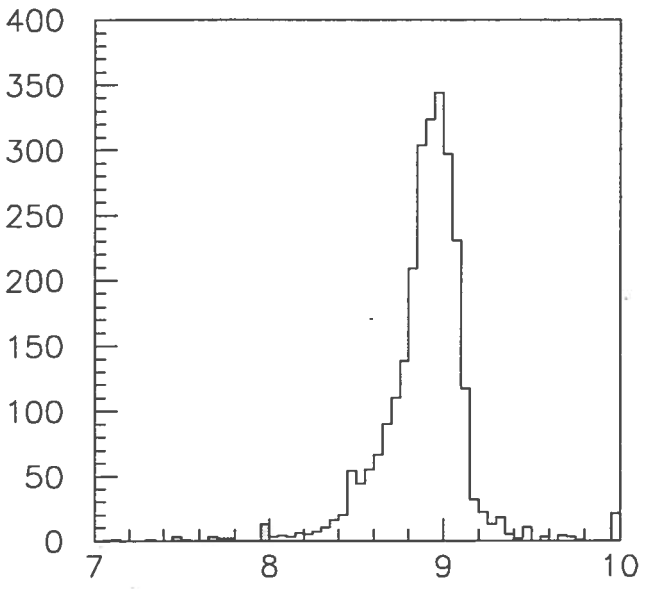

Avg. Strip Hits, Dec. 1992 – Dec. 1994

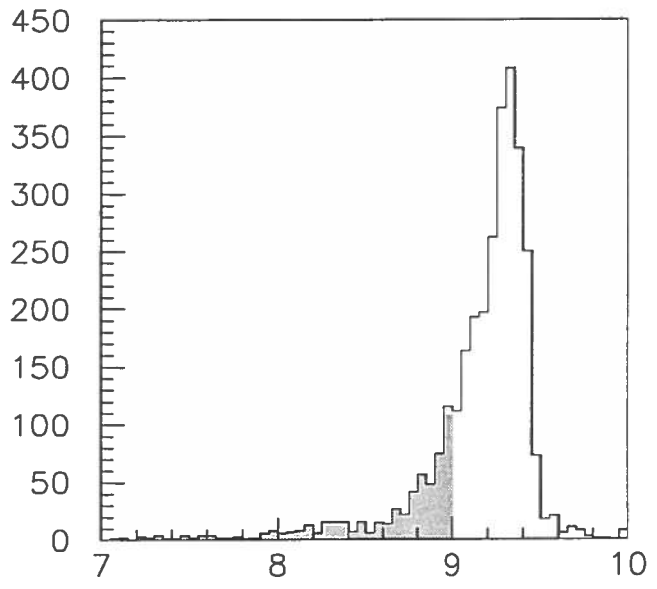

Avg. Wire Hits, Jan. 1991 – Nov. 1992

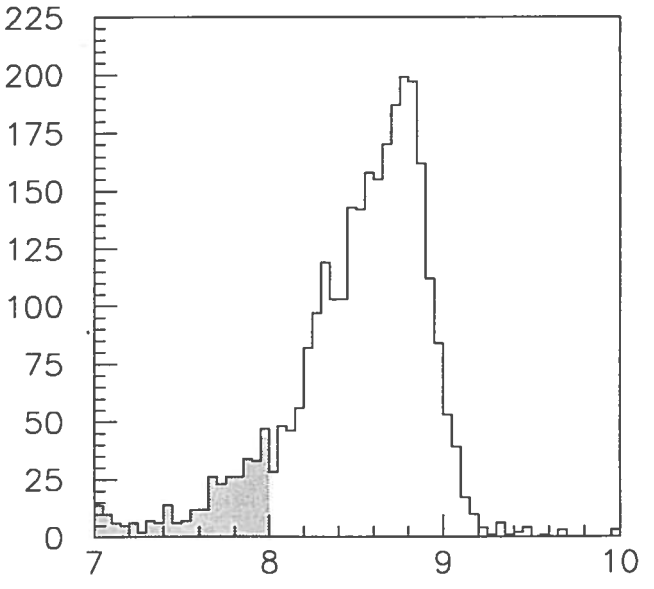

Avg. Strip Hits, Jan. 1991 – Nov. 1992

Figure 1

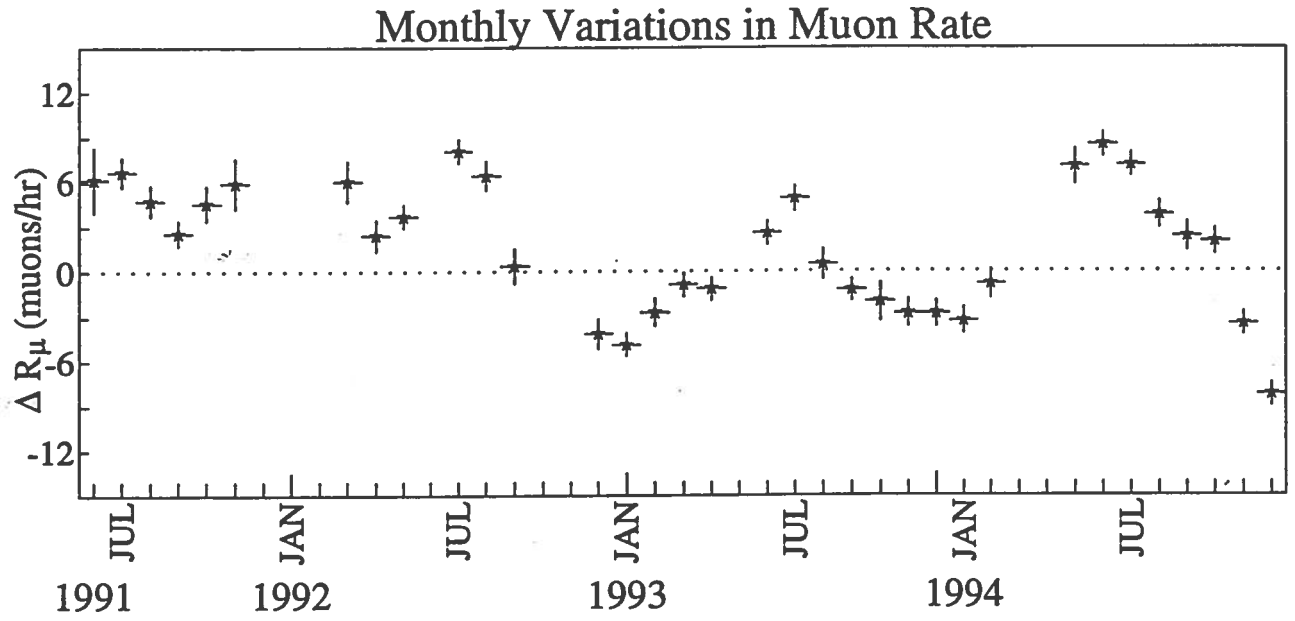

Figure 2

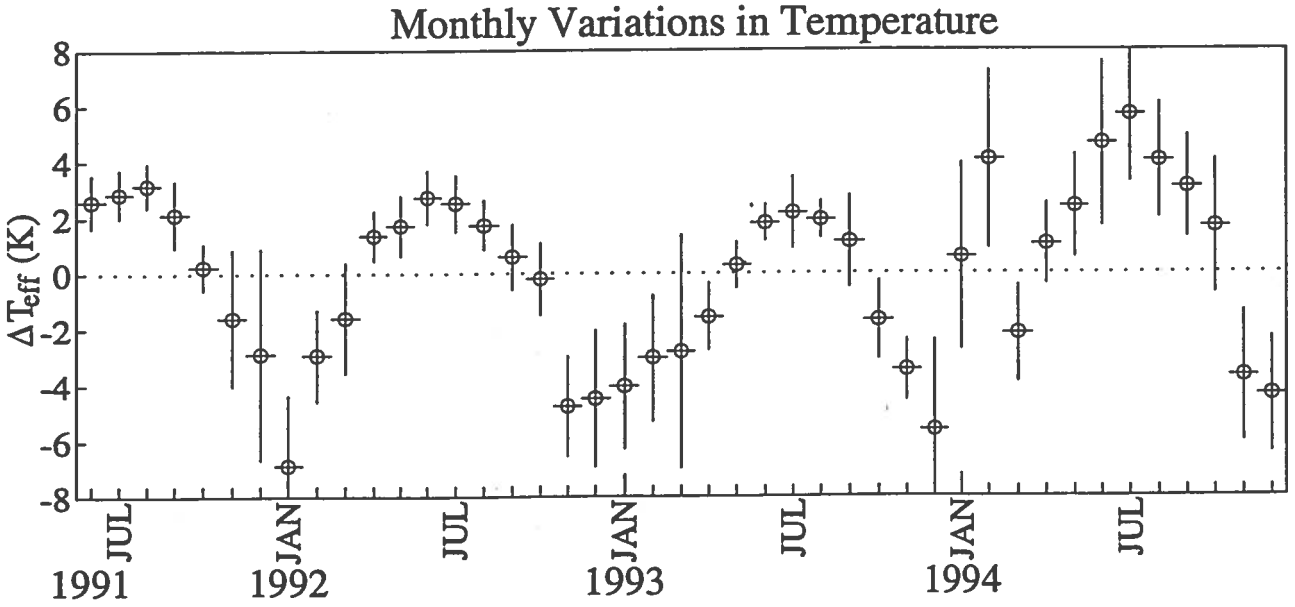

Figure 3

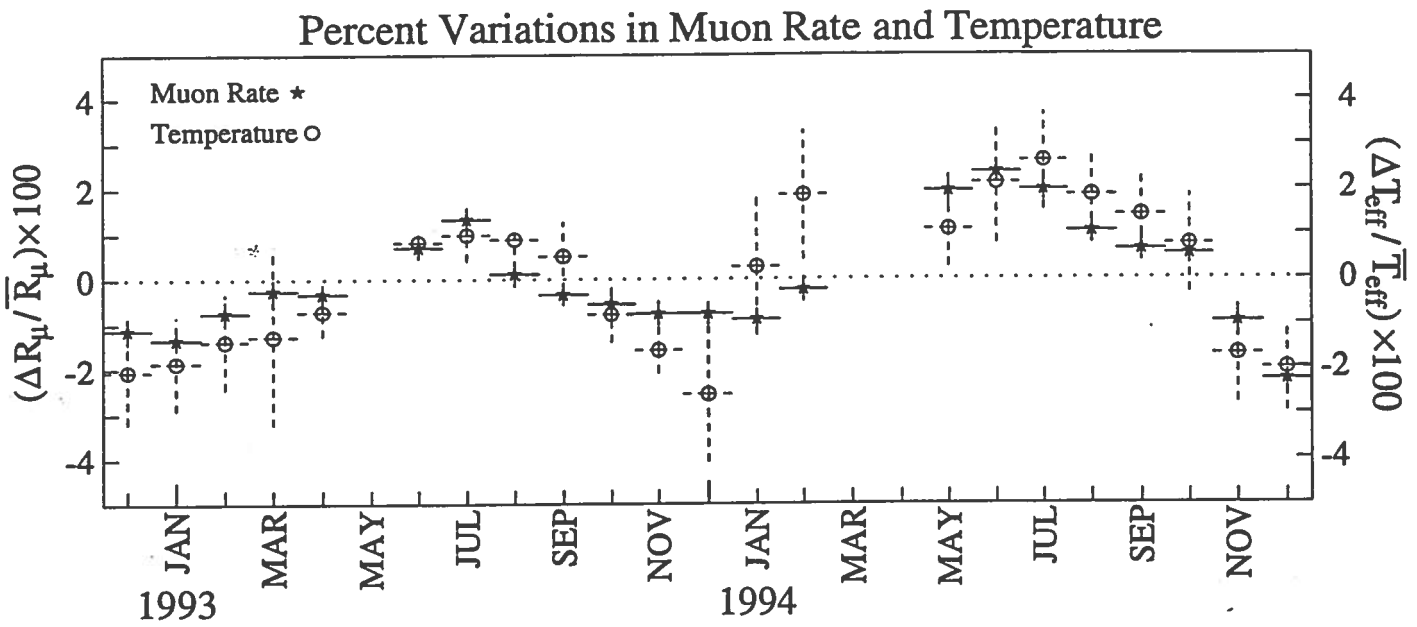

Figure 4

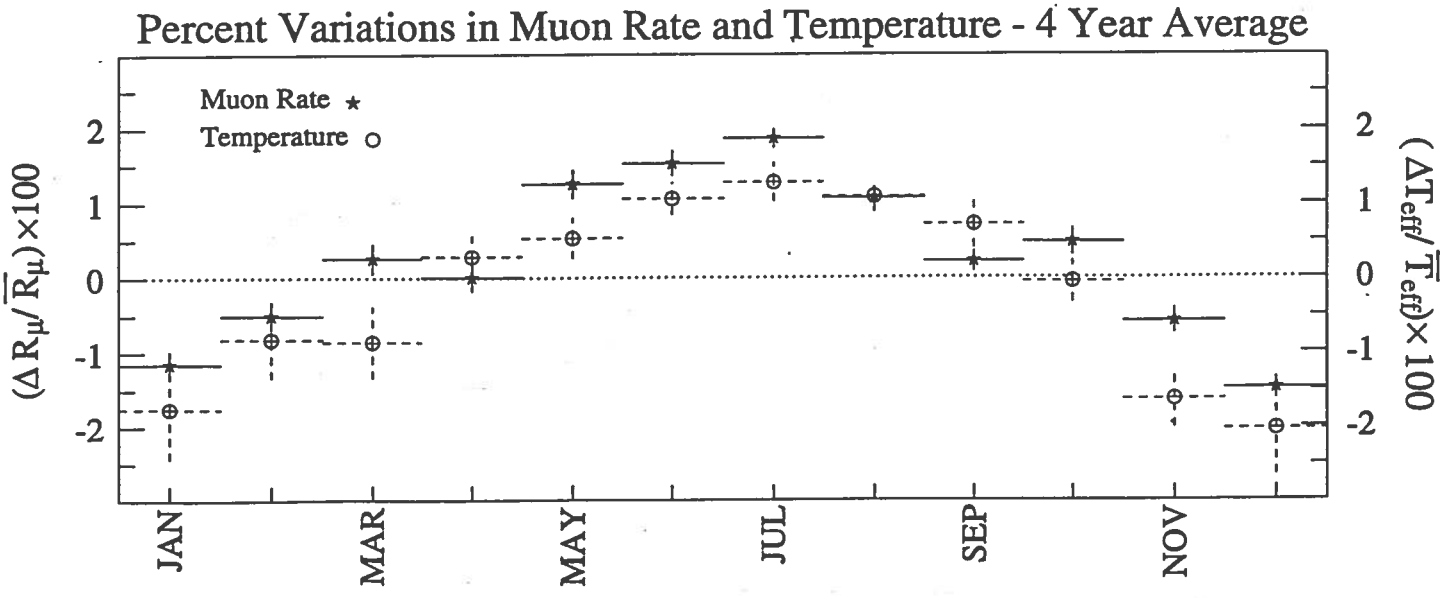

Figure 5

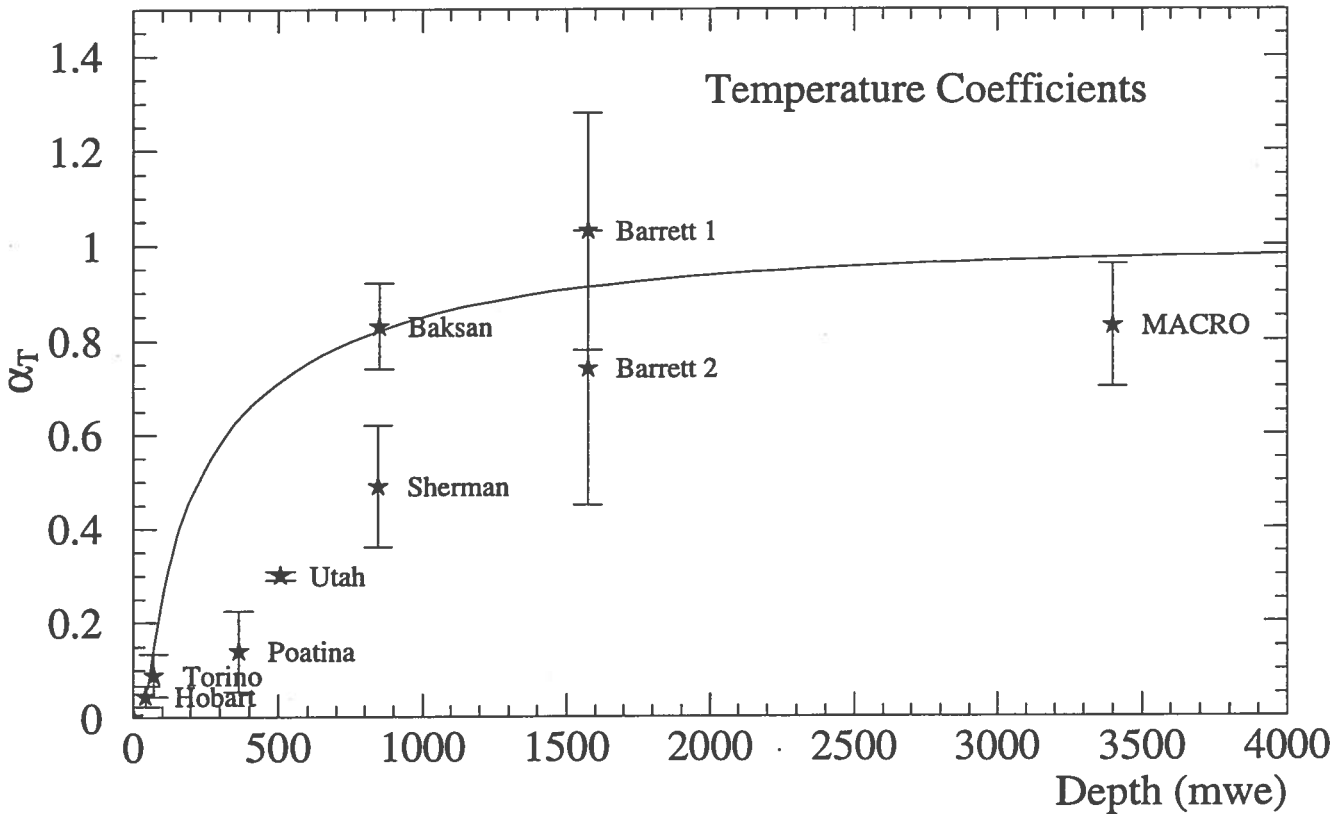
Temperature Coefficients
α_T
1.4
1.2
1
0.8
0.6
0.4
0.2
0
Barrett 1
Baksan
Barrett 2
MACRO
Sherman
Utah
Poatina
Torino
Hobart
0
500
1000
1500
2000
2500
3000
3500
4000
Depth (mwe)

Figure 6